Modelling two-stage antibiotic release from orthopedic fixation pins to prevent post-op osteomyelitis

Keywords: porous stainless steel, mesoporous silica beads, Linezolid, orthopedic fixation pin, 1D diffusion

BEE 4530 Computer-Aided Engineering: Applications to Biological Processes

© Asmita Bhatta, Matthew Jundong Kim, Melanie Lim, Rory Sheng

May 7, 2019

Contents

1 Executive Summary **2**

2 Introduction **3**

3 Problem Statement **5**
3.1 Design Objectives 5
3.2 Schematic 6
3.3 Qualitative Description of the Process 7

4 Governing Equations and Boundary Conditions **8**
4.1 Governing Equations 8
4.2 Boundary and Initial Conditions 9

5 Results **10**

6 Discussion **12**
6.1 Validation 12
6.2 Sensitivity Analysis 13
6.3 Optimization 14

7 Conclusions and Recommendations **16**
7.1 Design Constraints and Considerations 16
7.2 Future Recommendations and Improvements 17

Appendices
A Mathematical Statement of the Problem **19**
A.1 Exact Form of Governing Equation 19
A.2 Exact Form of Initial and Boundary Conditions 20
A.3 Drug and SBF Parameters and Constants 21
B Solution Strategy **22**
B.1 Computational Methods 22
B.2 Mesh 22
B.3 CPU Time Taken and Memory Used by a Typical Run 23
C Parameter Calculations **24**
D References **26**

1 Executive Summary

The first six hours following orthopedic implantation is a decisive period for preventing bacterial adhesion to ensure an implant's long-term success. If bacterial adhesion is not adequately impeded, a biofilm will form, acting as a diffusion barrier to slow down the implant integration process. Current therapies to treat osteomyelitis and other forms of implant-related infections include physical removal of the infected device, revision surgery, and prolonged antibiotic therapy. However, osteomyelitis still occurs at significant rates, and affected patients often require surgical adjustment or systemic antibiotic dosages.

This project considers a cylindrical drug-eluting pin, comprised of a reservoir of packed mesoporous silica MCM-48 microparticles, where the antibiotic (linezolid) is adsorbed. As simulated body fluid flows into the pin, the drug is desorbed from the microparticles and diffuses down its concentration gradient to be released in a sustained manner. A one dimensional diffusive mass transport simulation in COMSOL 5.3 Multiphysics was used to quantitatively simulate this process with the objective of optimizing design options such as porosity and pin geometry with respect to drug delivery, specifically the concentration of the drug on the surface of the pin where bacterial adhesion occurs. We modeled a pin with 17% wall porosity packed with 440 nm silica beads. These dimensions can be altered to improve current fixation pin designs which can facilitate treatment procedures.

Our model exhibited higher rates of release when compared to the experimental data, with 50% of total drug release achieved at approximately 8.5 and 40 hours respectively. This can be explained by the limited volume of SBF used in the experiment in contrast to the "infinite" amount of SBF that was assumed in our model, leading to higher rates of diffusion and release in our computational model. Optimization of porosity revealed that 20% porosity leads to a drug release profile that maximizes the amount of time above the minimal bactericidal concentration (MBC) and minimal inhibitory concentration (MIC). In the design of future pins, since increases in porosity are associated with decreases in mechanical strength and increases in manufacturing costs, the resulting changes in the mechanical properties and manufacturing process are significant factors that must be taken into account when improving the existing design of orthopedic devices.

Keywords: porous stainless steel, mesoporous silica beads, linezolid, orthopedic fixation pin, 1D diffusion.

2 Introduction

Orthopedic devices designed to treat open fractures exhibit comparatively higher rates of infection than other types of orthopedic devices, due in part to the closer proximity of fractures to the skin surface [1]. Many current open fracture devices use fixation devices (e.g., pins, nails, and plates) directly connected to the bone for stabilization during the healing process. However, this connection between skin and tissue presents a critical entry point for bacteria and other infectious organisms. Implant-related infections account for 15% of all hospital-origin infections and are the most common types of infections among surgical patients [2]. While frequent cleansing of device pins can help attenuate bacterial infection, osteomyelitis (an infection of the bone) still occurs in open fractures at a rate that is significantly higher than in other types of orthopedic injury [3]. The first six hours following orthopedic implantation has been identified as the decisive period for preventing bacterial adhesion and is critical for an implant's long-term success [4]. If bacterial adhesion is not adequately impeded, a biofilm will form, acting as a diffusion barrier to slow down the penetration of nutrients and antimicrobial agents. As a result, treatment becomes much more difficult, with affected patients often requiring additional treatments including systemic antibiotic treatment or surgical adjustment [5].

Current research on medical therapies to treat bacterial adhesion and subsequent biofilm growth on medical implants have an overall success rate of 57% to 88% [6], and incur significant economic expenditures. Some of these therapies include the physical removal of the infected medical device, radical debridement or physical removal of the infected tissue, revision surgery, prolonged antibiotic therapy, and the use of anti-adhesive medical devices [6]. The invasive nature of debridement and revision surgery has driven the discovery of less detrimental techniques. Standard medical protocols to treat osteomyelitis, such as systemic delivery of antibiotics, suffer from drawbacks of systemic toxicity and poor penetration into target tissue. The prevention of orthopedic device-related infections (ODRI) through the development of anti-adhesive medical surfaces involves the coating of these device surfaces with compounds and antibiotics [7]. One strategy that uses a specific type of coating to prevent ODRI is the use of an ionic silver coating on the device surface. It is effective due to silver's broad spectrum of antibacterial activity in reducing infection rates. Another method is local antibiotic release from polymethyl methacrylate (PMMA)-based bone cements. However, a second surgery is required in this process to remove the PMMA beads, making this method non-ideal for the prevention of osteomyelitis [8]. In addition, prolonged antibiotic therapy can build up a patient's antibiotic resistance, leading to possible lifetime impairment. All of these factors make up the demand for advancement in ODRI research.

Since recognizing the need for local delivery of antibiotics immediately following implantation, more research has been conducted in identifying problems with the current systemic approach. Some issues with current prevention techniques include the poor penetration of antibiotics into ischemic and necrotic tissue [9]. This can be corrected by maintaining a high local drug concentration for a short period of time so as to prevent buildup of a toxic concentration in the overall system. The effectiveness of a system designed to prevent ODRI strongly depends on two factors. The first is the rate of release of the drug [9]. The rate of release can affect a variety of factors, including ease of management of the drug, development of antibiotic resistance, the probability of eradicating the infection, etc. The other major factor affecting the efficacy of the system is the sustained release of the drug [10]. The sustained release of the drug at an effective level is necessary to prevent infection by latent bacteria. Current prevention and treatment practices are not optimized for either factor,

creating the need for a new system to be implemented.

The modelling and analysis of the drug-eluting pin aims to maximize the efficiency of antibiotic release and decrease the risk of infection after surgical treatment of bones. As more drug-eluting orthopedic implants have been developed, a new subcategory emerged: drug-filled orthopedic implants. These implants utilize the hollow space inside the implant as reservoirs for drug delivery without compromising the structural integrity of the implant. They aim to eliminate local infections by initiating the controlled drug release promptly after surgery. So far, three different designs of drug-filled orthopedic fixation pins have been studied in *in vitro* and *in vivo* studies.

The first design is a stainless steel hollow tubular fixation pin with antibiotic powder packed in the interior space of the pin and several orifices drilled in the reservoir wall to allow drug release [11]. The second design alters the structure of the wall of the fixation pin to be porous, while the hollow space inside the pin is still packed with antibiotic powder [11]. The third design has the same porous wall design, but uses a bed of mesoporous silica particles with the antibiotic adsorbed onto them, replacing the antibiotic powder [8]. This particular pin design includes two sets of variables that can be controlled independently–the properties of the porous wall and the properties of the mesoporous silica particles [8]. The antibiotic is first released from the mesoporous silica particles when the tissue fluid enters the silica bead matrix. It then diffuses through the porous wall of the fixation pin into the surrounding liquid environment. This two-stage release offers greater flexibility for tailoring the drug release profile [12]. Bactericidal and mechanical studies were performed on the prototypes for this fixation pin design, and the drug release over time was recorded. This design is shown to provide a significant reduction of bacterial growth. However, in this study, Perez et al. [8] did not model the physics of the tissue fluid and drug diffusion into and out of the pin. In addition, the group was unable to successfully reproduce the constant fluid flow outside of the implant as in a real-life setting, instead using an *in vitro* setup with 100 mL of simulated body fluid (SBF) with stirring [12].

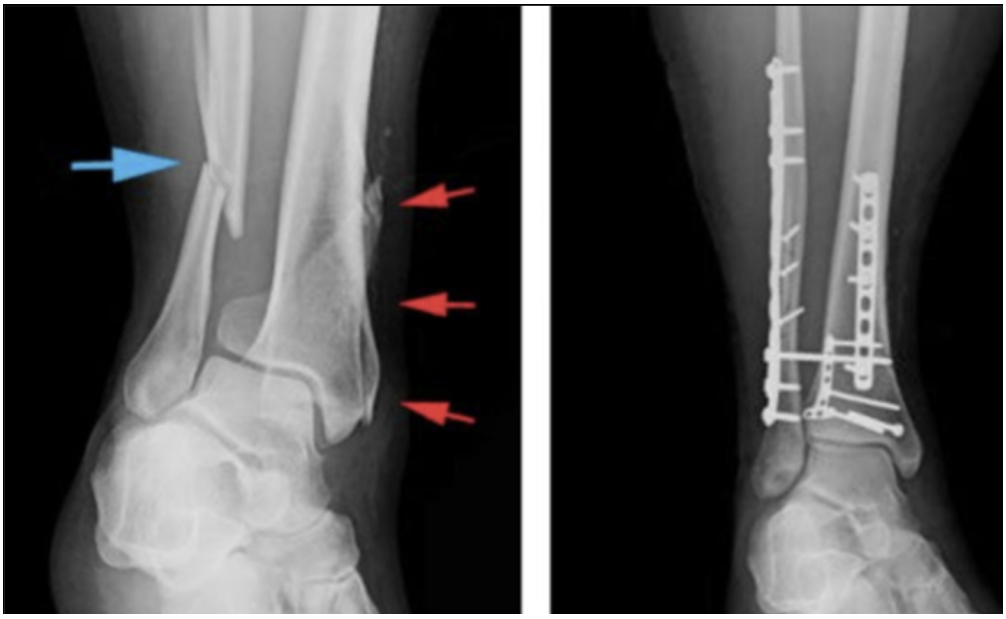

Figure 1: X-ray images showing fractures in the fibula and tibia shafts treated with plates and metal pins inserted into the plate frame to stabilize and realign the bone.

3 Problem Statement

Our project builds on the orthopedic fixation pin design proposed by Perez et al. [8]. The process being modeled is the diffusion of antibiotic particles that have been adsorbed onto mesoporous silica beads, packed in a hollow stainless steel orthopedic fixation pin. The drug is desorbed from the beads as the SBF diffuses into the silica bead matrix, and diffuses out through the porous steel wall into the simulated body fluid (SBF) outside the pin. This project will provide physical modeling to test the Perez et al.[8] implant design. It may also provide a basis for future directions to optimize the drug release profile by varying parameters such as the diameter and quantity of the silica beads, or the porosity of the beads or the pin wall without compromising the mechanical capabilities of the pin.

Given the complex nature of the problem, it is difficult to characterize the effects of varying fixation pin design parameters such as the porosity and thickness of the titanium wall and initial concentration of drug loaded onto the silica matrix on the release kinetics of the antibiotic, Linezolid. Prior *in vitro* and *in vivo* experiments do not provide information on the effects of these parameters on drug release. Without detailed characterization of the device, further design optimization is difficult. *In vivo* experiments are costly and time consuming, requiring numerous trials, and thus are not generally feasible for design studies. Computational modeling, on the other hand, is far less resource demanding, and allows users to easily tweak and alter parameters in order to quantify the effects on the system of interest.

3.1 Design Objectives

The primary objective of modeling this system in COMSOL was to optimize the time taken to release all of the drug adsorbed on the mesoporous silica bead matrix by varying parameters throughout the drug release process without compromising the mechanical properties of the fixation pin. Our initial computation measures the change in concentration of SBF as it diffuses through the porous stainless steel pin wall and through the mesoporous silica bead matrix at the center of the pin. The change in concentration of the drug as it diffuses out of the silica matrix and out of the porous pin wall is also measured simultaneously. By varying combinations of both SBF diffusivity values and drug diffusivity values in the wall and the matrix, we can compare the results over a period of time. A minimum concentration of the drug must be released within the first six hours to inhibit the formation of a biofilm, and the drug should have a sustained release period following the initial release phase. Therefore, to optimize the given system, the effects of design parameters such as porosity, wall thickness, and initial drug concentration are compared with the objective of minimizing the time taken to reach the critical bactericidal drug concentration required. In modeling this process, we hope to:

1. Compute sensitivity of release kinetics to fixation pin design parameters (e.g. porosity, wall thickness, initial drug concentration).

2. Determine in isolation the sensitivity of release kinetics to changes in material properties, such as diffusivity.

3. Compare the relative sensitivities to fixation pin design parameters and changes in material properties to make a concrete claim regarding which combination of parameters is the most

important in achieving a drug release profile capable of inhibiting formation of a biofilm.

3.2 Schematic

This cylindrical drug-eluting pin is comprised of a reservoir of packed mesoporous silica MCM-48 microparticles contained within the porous 316L stainless steel wall, as shown in Figure 2. Linezolid, a synthetic antibiotic, has been adsorbed onto the silica beads prior to the assembly of the pin. One end of the pin is sealed with a blind end cap, while the other end is capped with a polytetrafluoroethylene (PTFE) conical plug after the drug-loaded silica beads have been loaded [8]. The initial conditions and boundary conditions for our system are noted in section 5.0 on a figure of the schematic (Figure 3) and the exact equations are noted in Appendix A2. The governing equations are discussed in section 4.0.

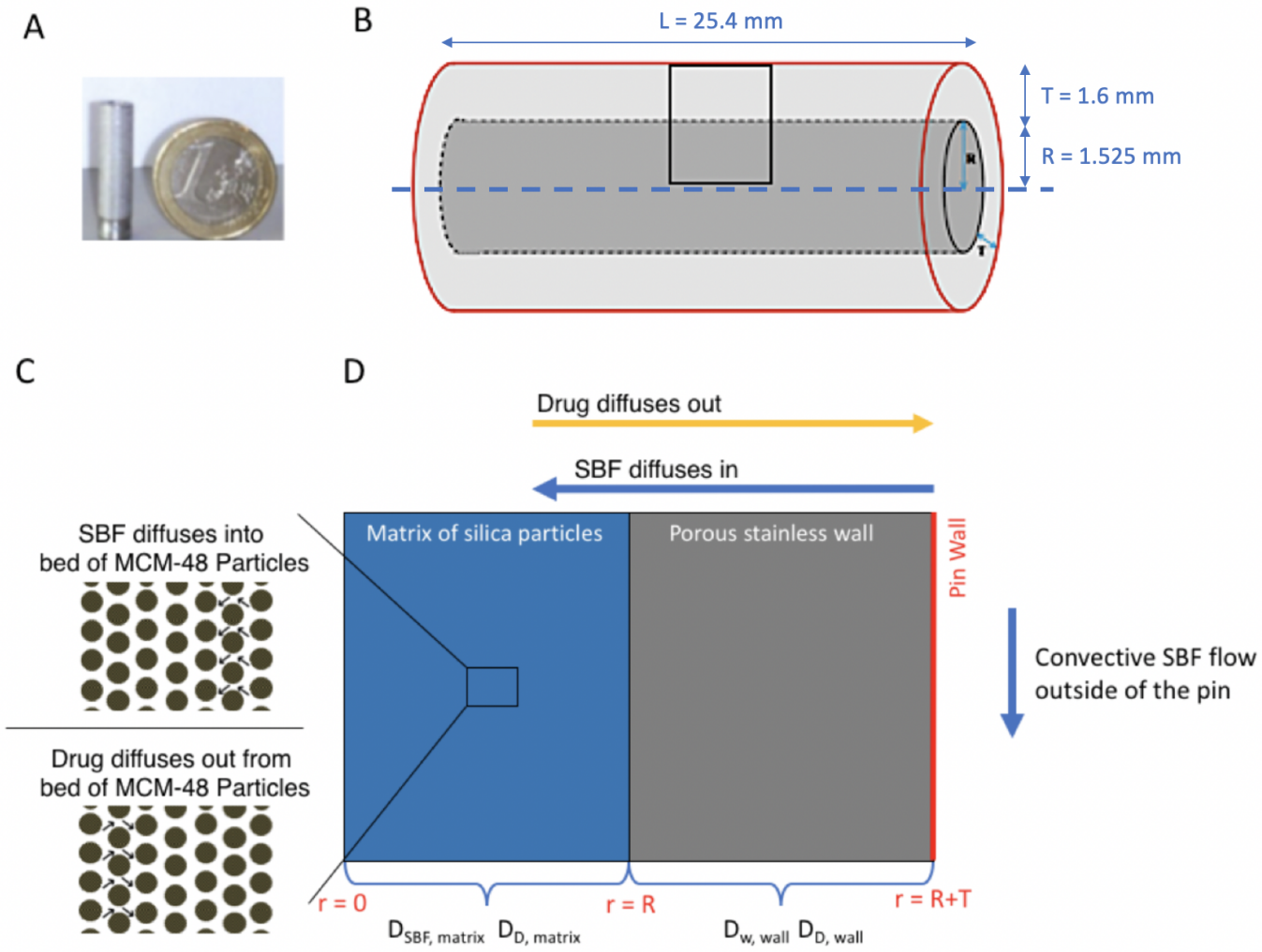

Figure 2: (A) Size comparison between the drug-eluting pin next to a 1 coin. [8] (B Simplified schematic of the two-domain system of one drug-eluting pin that was modeled in COMSOL. (C) The physics of the SBF and linezolid diffusions through the porous wall and silica beads. (D) Arrangement of mesoporous silica beads inside the cylinder [13].

The dimensions and designed material properties of the pin, porous stainless steel wall, and mesoporous silica MCM-48 microparticles are recorded in Table 1.

Table 1: Dimensions and Properties of the Hollow-Porous Pin

	Dimension	Value
Pin	Outer diameter	6.25 mm
	Outer radius	3.125 mm
	Length	25.4 mm
	Inner radius	1.525 mm
Porous wall	Porosity of wall	17%
	Thickness of wall	1.6 mm
	Nominal pore size	200 nm
Silica beads	Bead diameter	440 nm
	Average pore diameter	3.49 nm

3.3 Qualitative Description of the Process

The cylindrical drug-eluting pin is modeled as a 1D diffusion problem implemented as 2D axisymmetric along the entire length of the pin due to axial symmetry along the z-axis. The antibiotic Linezolid is adsorbed onto spherical mesoporous silica particles, which are packed into a hollow pin with a porous stainless steel wall. The packed pins are then immersed into simulated body fluid (SBF) which diffuses into the pin through the porous wall. The drug is eluted from the silica beads. The drug migrates through the silica particles, then exits the pin through the porous wall by simple capillary diffusion, where it is ultimately released into the surrounding body fluid.

4 Governing Equations and Boundary Conditions

4.1 Governing Equations

The mass transfer physics are used to model two species – linezolid and SBF. As shown in Figure 2, the modeling system contains two domains –the inner matrix made of drug-containing silica particles and the porous stainless steel wall. The drug and SBF concentrations at the interface between the two domains are continuous, so no boundary condition was required. The process is modeled for *in vitro* testing of the drug-eluting pin [8].

Both mass transfer processes are modeled as one dimensional transient diffusion in the radial direction. The axisymmetry of the pin simplifies the model to a two dimensional geometry. The consistent drug concentration throughout the matrix of the pin reduces any significant differences in the axial direction, thus making this a one dimensional problem. The SBF diffuses through the porous wall and the inner matrix made of silica beads. The drug, linezolid, diffuses out of the inner matrix and the porous wall as SBF enters. The governing equations used for SBF and drug diffusions are listed below.

SBF diffusion:
[0 <r <R]

$$\frac{\delta C_{SBF}}{\delta t} = D_{SBF,matrix}\left(\frac{1}{r}\frac{\delta}{\delta r}\left(r\frac{\delta C_{SBF}}{\delta r}\right)\right) \tag{1}$$

[R <r <(R+T)]

$$\frac{\delta C_{SBF}}{\delta t} = D_{SBF,wall}\left(\frac{1}{r}\frac{\delta}{\delta r}\left(r\frac{\delta C_{SBF}}{\delta r}\right)\right) \tag{2}$$

Drug diffusion:
[0 <r <R]

$$\frac{\delta C_{D}}{\delta t} = D_{D,matrix}\left(\frac{1}{r}\frac{\delta}{\delta r}\left(r\frac{\delta C_{D}}{\delta r}\right)\right) \tag{3}$$

[R <r <(R+T)]

$$\frac{\delta C_{D}}{\delta t} = D_{D,wall}\left(\frac{1}{r}\frac{\delta}{\delta r}\left(r\frac{\delta C_{D}}{\delta r}\right)\right) \tag{4}$$

Meanwhile, the drug diffusivity and SBF diffusivity values in the matrix depend on changes in SBF concentration in the matrix. They are calculated based on the following equations found in [14].

SBF diffusivity through silica beads (matrix):

$$D_{SBF,matrix} = D_{SBF,eq}e^{-\beta_1\left(1-\frac{C_{SBF}}{C_{SBF,eq}}\right)} \tag{5}$$

Drug diffusivity through silica beads (matrix):

$$D_{D,matrix} = D_{D,eq}e^{-\beta_2\left(1-\frac{C_{SBF}}{C_{SBF,eq}}\right)} \tag{6}$$

Table 2: Symbols used in the governing equations.

Variables and Solvers	
SBF Concentration	C_{SBF}
Drug Concentration	C_D
Radial distance from the central axis of the cylindrical pin	r
Time starting with SBF entering the porous steel wall	t
Diffusivity of drug through the silica beads in the inner cylinder	$D_{D,matrix}$
Diffusivity of SBF through the silica beads in the inner cylinder	$D_{SBF,matrix}$

4.2 Boundary and Initial Conditions

The geometry is simplified as a 2D axisymmetric model about the central axis of the drug-eluting pin. For the top surface sealed by the PTFE cap and the bottom sealed surface of the pin, the diffusive flux equals zero. Because the external SBF solution is being stirred, the boundary condition of drug diffusion is the outward flux due to the convective SBF flow along the right outer wall surface in Figure 3 below.

The initial conditions for the model designate an initial drug concentration within the silica bead matrix on the left, while there is no initial concentration of either drug or SBF throughout the rest of the model. The exact equations used for the initial and boundary conditions are noted in Appendix A2.

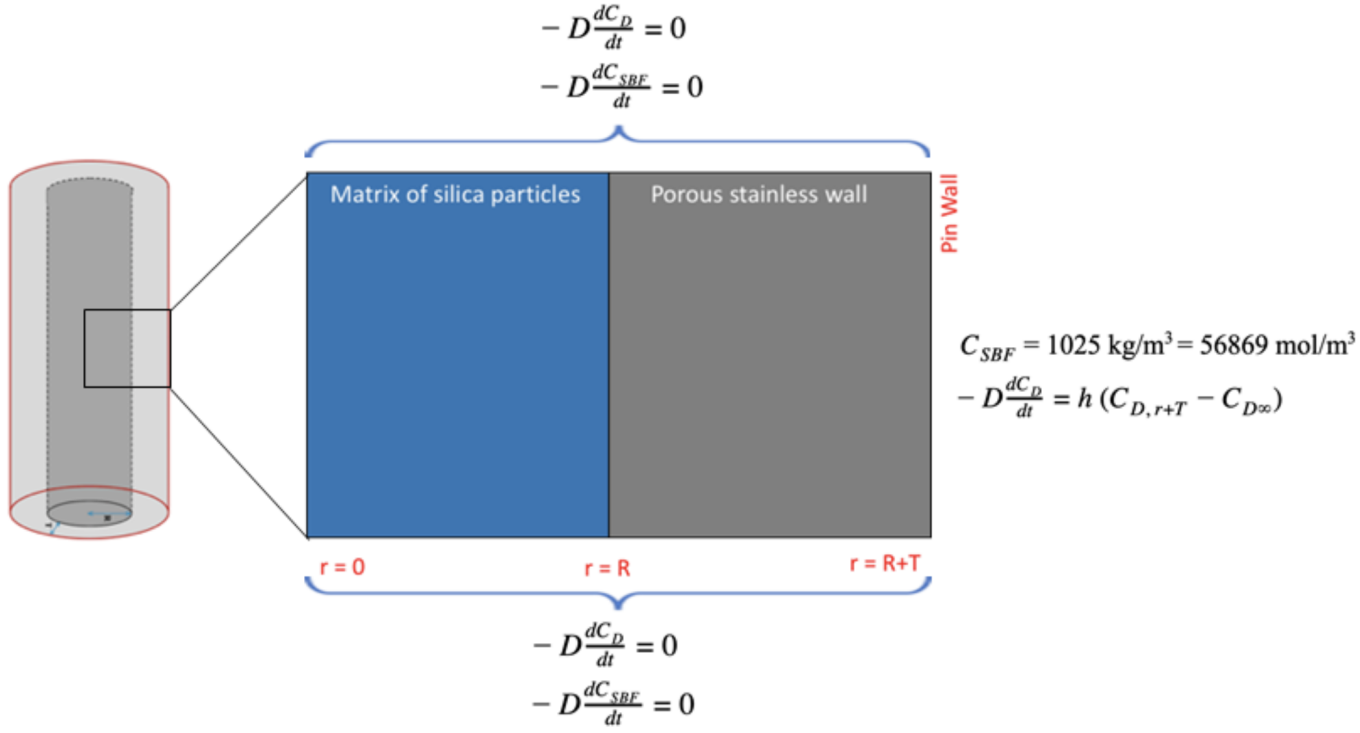

Figure 3: Simplified schematic and boundary conditions for the model are shown.

5 Results

Obtaining a drug concentration above the MIC and MBC values ensures that the concentration of antibiotic released is able to effectively prevent the growth of bacteria. To evaluate the calculated solution in COMSOL, the following graph was created to show the drug concentration release over a time period of 160 hours. The MIC and MBC values are indicated with the red and green horizontal lines. The drug concentration exceeds the minimum concentration needed to treat the bacteria within the first 5-160 hours of release.

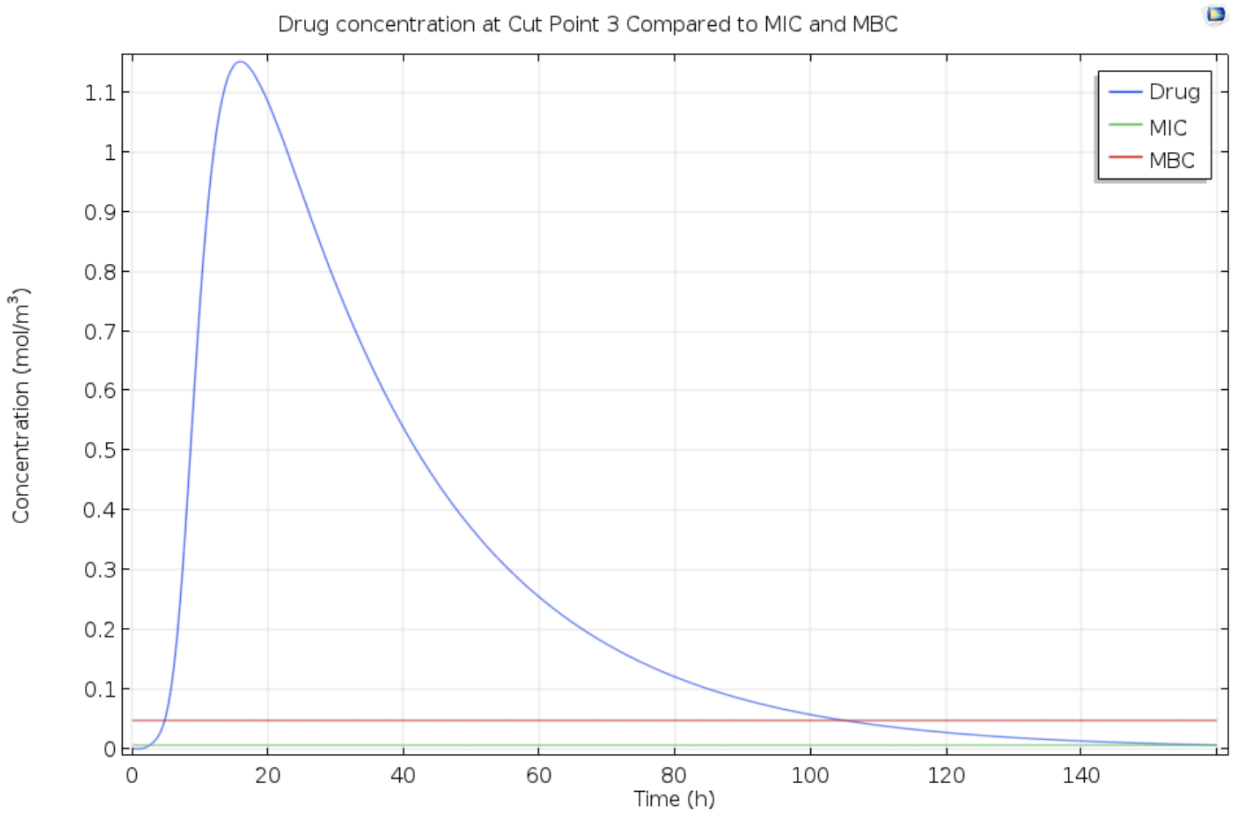

Figure 4: Drug concentration at the wall of the pin over time with MIC (0.00593 mol/m^3) and MBC (0.04743 mol/m^3) values shown

In Figure 4, the drug concentration over time at the wall of the pin initially increased as the drug releases from the inner silica bead matrix. After about 20 hours, the drug concentration at the wall experienced a first order decrease. During the initial few hours, the drug concentration at the wall rapidly surpassed the MIC of 0.00593 mol/m^3, and the MBC of 0.04743 mol/m^3. This desired high antibiotic concentration remained until about the 100th hour for MBC and about the 160th hour for MIC. In addition to monitoring the amount of drug concentration that effectively prevents bacterial growth, we ensured that the total amount of linezolid contained inside the pin does not approach the toxic level for this drug within the body even if all of the drug were released at once [8].

This modeling result is consistent with the sustained release indicated by the Perez et al. [8] study. We can visualize the drug concentration profiles from the central axis of the fixation pin to the wall at different times of the drug release process (Figure 5). Initially, all of the drug concentration

was contained in the silica matrix while the porous stainless steel wall had no drug. As time went on, the inside drug concentration decreased as the drug diffused out through the SBF in the matrix and the porous wall, and was carried away by the convective flow outside of the pin.

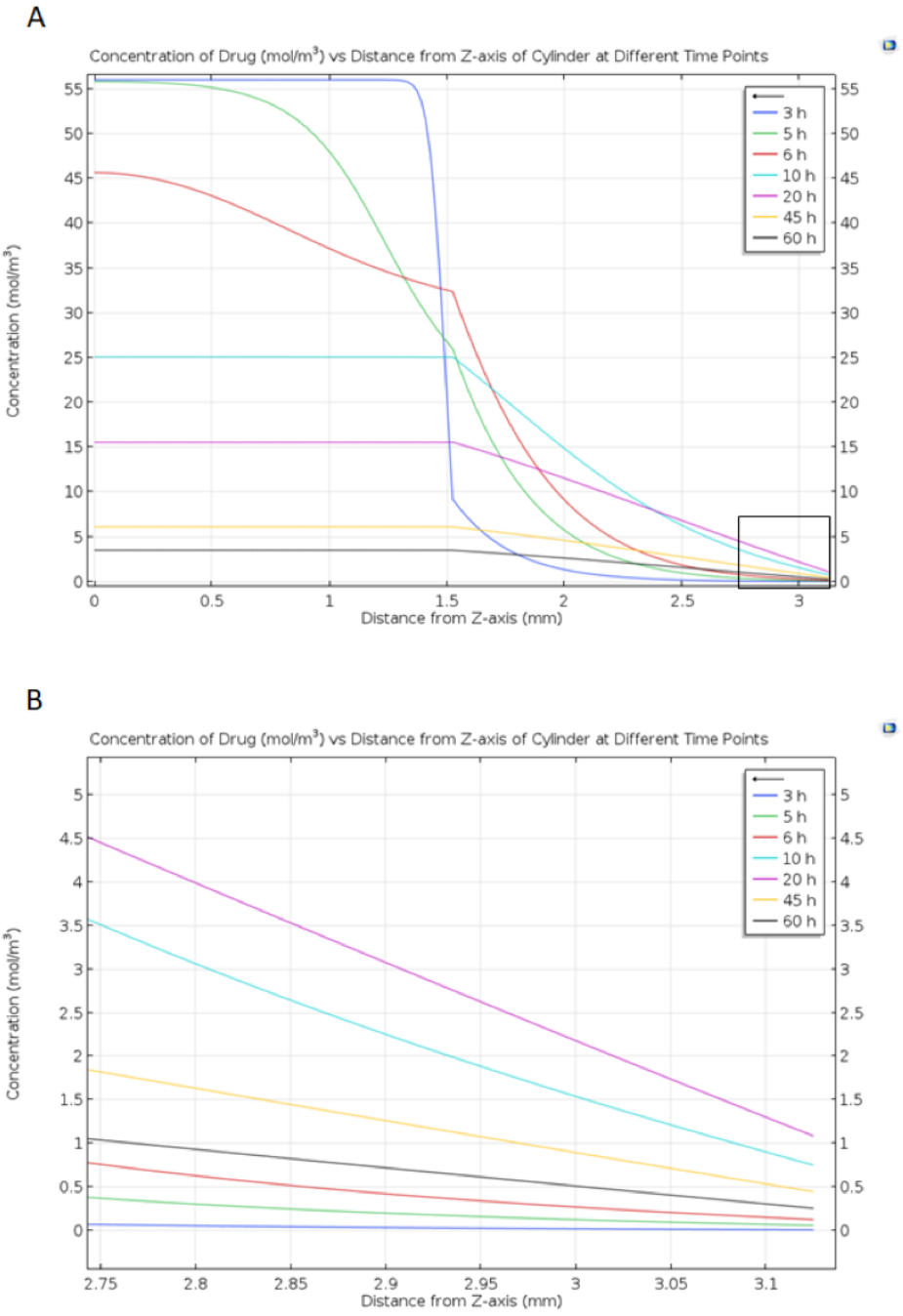

Figure 5: (A) Drug concentration plotted over distance from the central axis of the pin to the wall, at different times. (B) Zoomed in section showing the decrease in drug concentration profile over time close to the outside of the porous steel wall.

6 Discussion

6.1 Validation

Comparing the results of our simulated drug release to the results from literature Perez et al. [8], the linezolid release profile over time appears similar. Figure 6 below shows that the drug release from the experimental data is slower compared to the values we computed. This can be accounted for by the limited volume of SBF used in the *in vitro* experiment in contrast to the "infinite" amount of SBF that we have assumed in our model. The experiment uses 100 mL of SBF which will slowly become saturated with the drug, resulting in a slower release rate. In our model the SBF outside the pin is stirred and constantly renovated, preventing the accumulation of linezolid in the fluid around the pin. Our model is more similar to the *in vivo* set up for the pin where the tissue fluid would be constantly circulated, maintaining a steep gradient for the drug release from the pin.

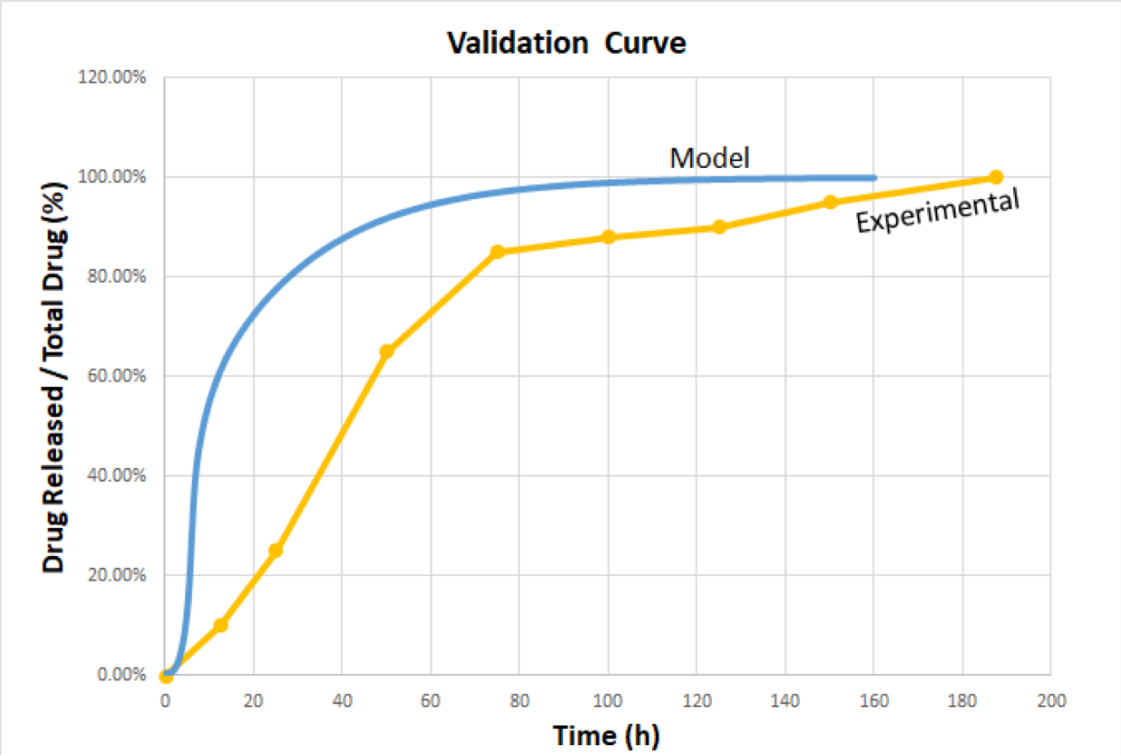

Figure 6: Linezolid released as a percentage of linezolid initially loaded into the pin for the computed data using our model and the experimental data from Perez et al. [8].

The objective of this device is to prevent bacteria film formation during the critical period (first six hours after implantation), and to continue to inhibit and control bacterial growth 48 hours after implantation [8]. Thus, the drug concentration in the wall should be above the minimum bactericidal concentration (MBC) for at least the critical period, and above the minimum inhibitory concentration (MIC) for the growth of bacteria up to a minimum of 48 hours after implantation. For the bacterium *Staphylococcus aureus*, the MBC and MIC are 0.04743 mol/m^3 and 0.00593 mol/m^3 respectively. Our model is consistent with these values based on the data obtained to generate Figure 4 which shows the concentration of the drug at cut point 2, very close to the exterior

of the pin.

6.2 Sensitivity Analysis

Sensitivity analyses were performed by observing how the results of the model change due to uncertainty in input parameters (e.g., $D_{D,SBF}$, $D_{SBF,wall}$, $D_{D,wall}$, etc.). To accomplish this, literature values of parameters of interest were varied by 10% and the percent changes in final concentration of the model results were observed. Specifically, the changes in concentration at the surface of the pin, six hours after the pin has been implanted, were observed. The first six hours are critical in the prevention of bacterial film formation, which is the root of orthopedic post-op infections. The concentration of the drug at the interface between the outer wall of the steel pin and the surrounding SBF determines if the drug will kill, inhibit the growth of, or allow propagation of the bacteria. For an initial examination of the model's sensitivity to variations in various diffusivities, we varied $D_{D,eq}$, $D_{SBF,eq}$, $D_{SBF,wall}$, $D_{D,wall}$, and h_{out} (see Table 3 in Appendix A.3 for definitions) by 10% at the surface of the pin at t = 6 h.

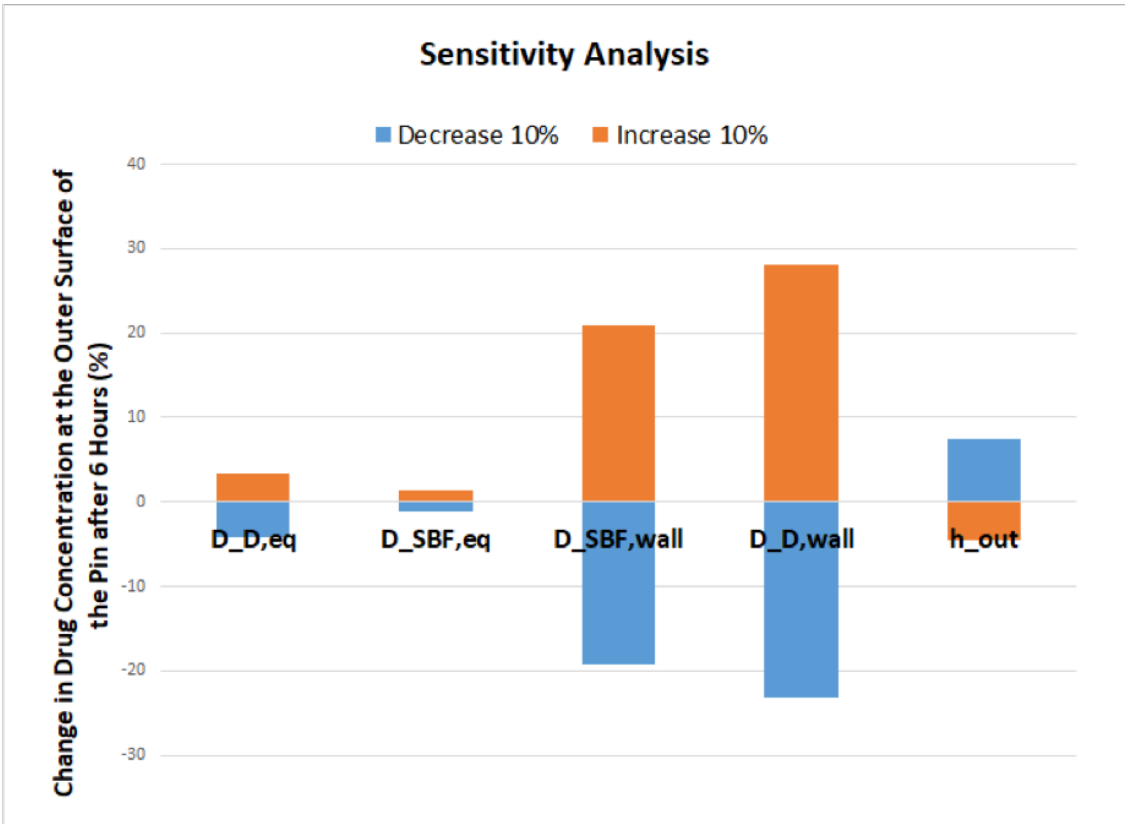

Figure 7: Sensitivity analysis of 10% change in drug and SBF equilibrium concentrations at the porous wall.

The largest change in solution result occurred due to changes in $D_{SBF,wall}$ and $D_{D,wall}$. A The largest change in drug concentration occurred due to changes in $D_{SBF,wall}$ and $D_{D,wall}$. A decrease and an increase of 10% of $D_{SBF,wall}$ led to a 19.15% decrease and a 20.96% increase respectively. Similarly, a decrease and an increase of 10% of $D_{SBF,wall}$ led to a 23.09% decrease and a 28.06%

increase respectively. Of the parameters examined above, our model exhibits the greatest sensitivity to changes in $D_{SBF,wall}$ and $D_{D,wall}$.

6.3 Optimization

The drug concentration on the outside surface of the pin is the most important variable to prevent bacterial infection. For the purposes of explaining our optimization process, this concentration shall be referred to as C_{drug}. There are two time points that are essential for this process to be at maximum efficiency: the time point at which C_{drug} exceeds the minimum bactericidal concentration (MBC), referred to as t1; and the time point at which C_{drug} falls below the minimum inhibitory concentration (MIC), referred to as t2. The ideal system would minimize t1, thereby allowing the bacteria very little time to form a film on the pin's surface, while maximizing t2, inhibiting bacterial growth for long periods of time after implantation. Finally, t1 needs to be positioned within the first six hours after implantation, since that is the period in which the pin is most vulnerable to bacterial adhesion and film formation, which can later lead to infection [4]. The material property we chose to vary to achieve these changes in t1 and t2 was porosity. We quantified this ideal behavior using three functions:

$$F_1(\text{t}) = \text{t1 for c} > \text{MBC; 0 for c} < \text{MBC} \tag{7}$$

$$F_2\ (\text{t} = 6\text{hrs}) = 1 \text{ for c} > \text{MBC; 0 for c} < \text{MBC} \tag{8}$$

$$F_3(\text{t}) = \text{t2 for c} > \text{MIC; 0 for c} < \text{MIC} \tag{9}$$

Here, F_1 can be used to minimize t1, F_2 ensures that t1 occurs within the first six hours, and F_3 can be used to maximize t2. The three functions were combined to form an objective function that could be maximized to find an optimal porosity for the porous steel wall of the pin, shown below:

$$\text{J} = F_2\ (F_1 + 10{*}F_3) \tag{10}$$

Here, F_3 is given a weight of 10 to ensure that the value of J is not determined by the absolute difference between t1 and t2, but rather by the individual values of the two times. We chose to weight F_3 more heavily because maximizing t2 would be more effective in preventing bacterial propagation, rather than minimizing t1; C_{drug} continues to decimate the bacteria while it stays above the MBC, which it does for the majority of the experiment, as can be seen from Figure 4. The variation of the objective function with respect to porosity is shown in Figure 8.

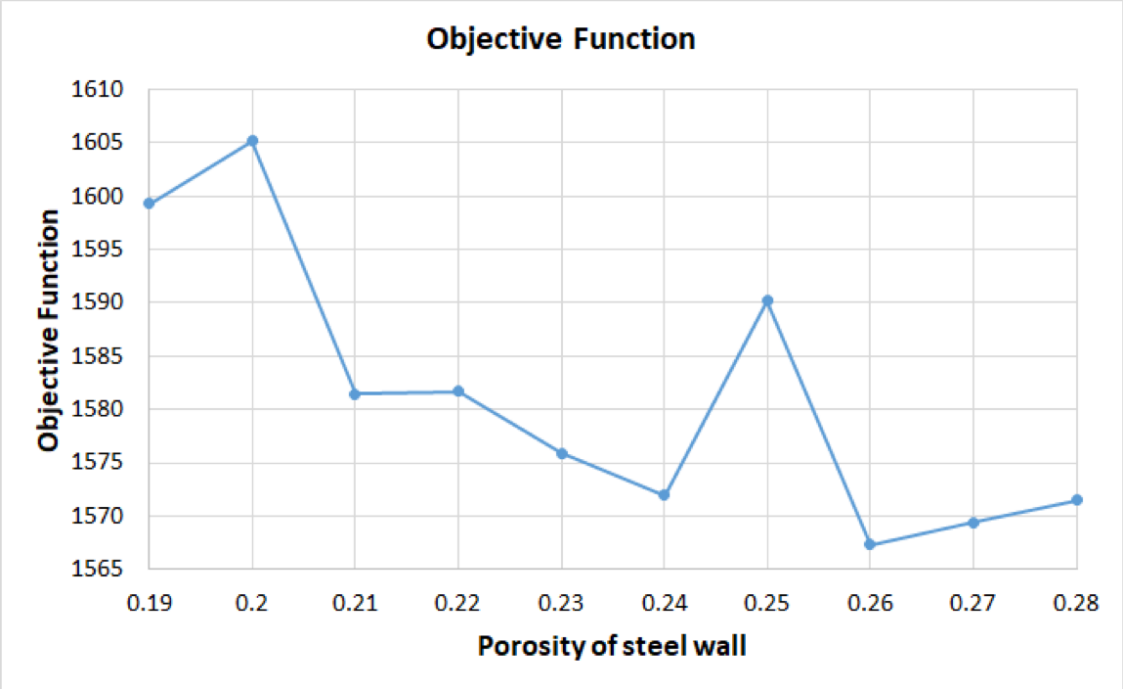

Figure 8: The objective function is maximized at 20% porosity of the stainless steel wall.

7 Conclusions and Recommendations

According to the sensitivity analyses conducted on the solution results, we decided to focus specifically on the sensitivity of our model to variations in $D_{SBF,wall}$ and $D_{D,wall}$. The preliminary calculations of these values are shown in Appendix C, using the equation for the diffusion of a solute in a saturated porous system presented in [15]. Through this relationship, we observed that the diffusivity values could be altered most effectively by varying the porosity values within our model.

By implementing an objective function that determines the optimal porosity for the porous steel wall of the pin, we were able to address our final design objective of determining an optimal combination of parameters for a drug release profile that best inhibits biofilm formation.

The results of the maximized objective function indicate that the optimal design occurs at 20% porosity, yielding a drug release profile with the greatest range of time above the MBC and MIC values. The initial concentration of drug release rises to about 22 times the MBC value as seen in Figure 4, indicating that the Linzeolid concentration far exceeds the required bactericidal concentration value within the first 24 hours. To further improve this system, we decided to focus on maximizing the amount of time that the drug continues to remain above the MIC value over a long period of time, as shown in the objective function. By optimizing the amount of time during which the drug successfully inhibits bacterial propagation while maintaining a sufficiently high initial drug release profile within the first six critical hours, we are able to apply this optimal porosity value of 20% to the design parameters for the porous pin wall.

7.1 Design Constraints and Considerations

Use of these hollow porous stainless steel pins for orthopedic applications means they must be able to withstand the significant mechanical stresses associated with both normal and active movement. The porous steel pin used in this experiment could withstand compressive stresses of up to 300 MPa without plastic deformation [8]. For reference, the ultimate compressive stress supported by human bones has been estimated to be 196 MPa [16]. Thus, any alterations in the design of the pin must be made with the pin's mechanical properties in mind. Since increases in porosity decreases the strength of the pin and leads to lower values for the ultimate compressive strength, attention must be paid to ensure that newly manufactured pins with altered porosity still possess the mechanical properties necessary to withstand physiological stresses.

In addition, increases in porosity means the stainless steel wall material is thinner. This leads to increased difficulty in manufacturing, as more care is required to ensure continuity and precision over all parameters [17]. The additional precision required in these cases leads to increases in cost associated with higher porosity pins. However, it is important to note that high porosity pins were found to improve osseointegration, as the surface area available for bone growth is increased. In summary, when adjusting porosity and pin geometry, the resulting changes in the mechanical properties and the manufacturing process are significant factors that must be taken into account. Since increases in porosity are associated with both higher cost and increased osseointegration potential, these two effects should be weighed accordingly to reach a final design decision.

7.2 Future Recommendations and Improvements

Our model of the linezolid release over the first 160 hours after implantation provides valuable insights to the drug eluting physics of the Perez et al. [8] fixation pin design. The drug release kinetics of the current design is highly sensitive to changes in the diffusivities of SBF and linezolid in the porous stainless steel. In comparison, the diffusivities of SBF and linezolid in the silica matrix have limited effects to the drug release kinetics. This modeling result suggests that the design of the pin wall is critical for achieving rapid release in the first six hours and maintaining sustained long-lasting release. Taking into account these optimization criteria, our objective function gives an optimal porosity of 20% for the pin wall for the current design.

Theoretically, a well-defined and well-controlled design for the drug-eluting fixation pin should follow a two-phase zeroth order release profile. In the first phase, a high constant release rate enables the drug concentration at the outer surface of the pin wall to quickly raise above MBC. In the second phase, a constant release rate of nearly zero should be maintained for an extended period of time to stabilize the drug concentration above MIC and within the therapeutic window for linezolid function.

In order to effectively characterize and improve upon the current design of the fixation pin, additional experiments are required. Our model has indicated that the current *in vitro* set up of the Perez et al. [8] drug release experiment requires improvements in order to more accurately represent the fluid flow conditions *in vivo* near the human bone. Instead of renovating SBF after 160 hours, the outside SBF should be flowing over the surface of the pin, generating convective flux on the surface of the pin wall. After improving experimental set up, a series of additional mass transfer tests should be performed to obtain the effective diffusivities of the SBF and linezolid in the silica matrix and in the porous wall. Additional material properties of the silica matrix and the pin wall should also be measured experimentally, to enable to more accurately mathematical modeling and more effective design modification.

For future modeling of the drug release process, an alternative computational model can be constructed and tested against ours for validity. In this model, SBF enters into the porous wall by capillary flow instead of simple diffusion. A small scale model is implemented to estimate the effective diffusivity of SBF as it flows through the interstitial spaces in between the silica beads, in addition to the changing effective diffusivity of linezolid with changing SBF concentration. This alternative model uses more accurate physics than the single diffusive mass transfer used in our current computational model; it takes into account the tortuosity of the fluid as it travels between the silica beads, as well as the fluid flow that can occur in the pores of the stainless steel wall. We were not able to implement this model because of a lack of data available for all the parameters required. Due to the sensitivity of the values with respect to the dimensions, the drug used, and the composition of the fluid (SBF), it is difficult to find accurate values for the exact specifications for our model. Thus, some experimental data would need to be obtained in the future before this alternative model can be implemented.

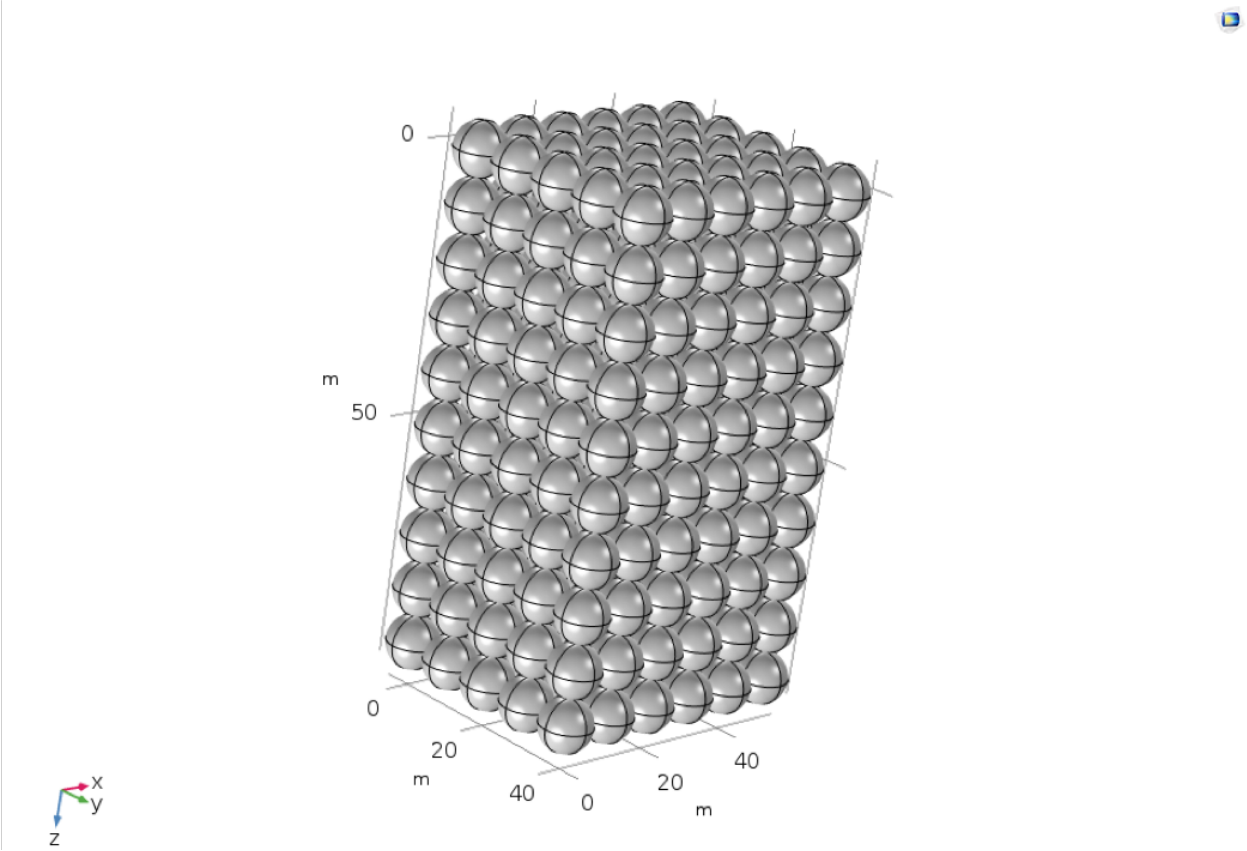

Figure 9: Potential geometry of the small-scale model. Mesoporous silica beads are tightly packed into an array.

This model can be used to test for the suitability of other materials to make the pin while the parameter values for properties associated with it can be obtained. One alternative could be titanium. Titanium has many biomedical applications, including orthopedic implants. Titanium orthopedic devices tend to be more costly compared to their stainless steel counterparts [18]. However, titanium has been found to cause less pain than stainless steel implants, and has a lower chance of loosening from the original location of implantation, a problem that leads to the premature removal of many orthopedic fixation pins [19]. Titanium has not been found to be more susceptible to bacterial infections compared to stainless steel [20]. The mechanical properties of the pin must also be taken into account. The diffusivity of linezolid and SBF would be different in the titanium pin, and may require a different porosity, which would affect the mechanical properties of the pin. Thus, without determining the pore sizes and porosity required for the pin, it is not possible to have an accurate comparison of the mechanical properties between the titanium pin and the stainless steel pin. Using this simulation or an improved version of it to test for the viability of a titanium implant of the same design would be one way to use this model to further improve treatment procedures.

Appendices

Appendix A: Mathematical statement of the problem

A1. Exact form of governing equation

As described and discussed in the Section 3.0, the exact form of governing equations used for SBF and drug diffusions in the silica matrix and in the porous stainless steel wall are listed below. Since these equations have been used earlier in the report, they retain their original numbers.

SBF diffusion:

[0 <r <R]

$$\frac{\delta C_{SBF}}{\delta t} = D_{SBF,matrix}\left(\frac{1}{r}\frac{\delta}{\delta r}\left(r\frac{\delta C_{SBF}}{\delta r}\right)\right) \tag{1}$$

[R <r <(R+T)]

$$\frac{\delta C_{SBF}}{\delta t} = D_{SBF,wall}\left(\frac{1}{r}\frac{\delta}{\delta r}\left(r\frac{\delta C_{SBF}}{\delta r}\right)\right) \tag{2}$$

Drug diffusion:

[0 <r <R]

$$\frac{\delta C_{D}}{\delta t} = D_{D,matrix}\left(\frac{1}{r}\frac{\delta}{\delta r}\left(r\frac{\delta C_{D}}{\delta r}\right)\right) \tag{3}$$

[R <r <(R+T)]

$$\frac{\delta C_{D}}{\delta t} = D_{D,wall}\left(\frac{1}{r}\frac{\delta}{\delta r}\left(r\frac{\delta C_{D}}{\delta r}\right)\right) \tag{4}$$

Meanwhile, the drug diffusivity and SBF diffusivity values in the matrix depend on changes in SBF concentration in the matrix. They are calculated based on the following equations found in [14].

SBF diffusivity through silica beads (matrix):

$$D_{SBF,matrix} = D_{SBF,eq}e^{-\beta_1\left(1-\frac{C_{SBF}}{C_{SBF,eq}}\right)} \tag{5}$$

Drug diffusivity through silica beads (matrix):

$$D_{D,matrix} = D_{D,eq}e^{-\beta_2\left(1-\frac{C_{SBF}}{C_{SBF,eq}}\right)} \tag{6}$$

A.2 Exact form of the initial and boundary conditions

As described in Section 4.0, the geometry is simplified as a 2D axisymmetric model with zero flux at the sealed PTFE cap of the pin, and the sealed bottom of the pin, and a convective convective flux boundary condition along the right outer wall surface.

For the porous wall,

$$\text{SBF concentration outside the pin: CSBF= 1025 kg/m3 = 56869 } mol/m^3 \tag{11}$$

Diffusion flux of drug:

$$-D\frac{\delta C_D}{\delta t} = h(C_{D,r+T} - C_{D\infty}) \tag{12}$$

The initial values are generated based on the loading situation of the drug and SBF inside the pin at time zero [t = 0].

[0 <r <R]:

$$C_D = C_{Di} \tag{13}$$

$$C_{SBF} = 0 \tag{14}$$

[R <r <(R+T)]:

$$C_D = 0 \tag{15}$$

$$C_{SBF} = 0 \tag{16}$$

A.3 Drug and SBF Parameters and Constants

Property/Parameter Name	Value	Notes	Source
Drug Parameters			
Initial concentration of the drug inside the silica beads C_{Di}	56.0146 mol/m^3	Original experiment done using prototype of the fixation pin	[8]
Diffusivity of drug in the equilibrium swollen state of the system $D_{D,eq}$	6.3 x $10^{-11} m^2/s$	Experimental data from drug-eluting HPMC tablets	[14]
Diffusivity of drug through the porous steel wall of the pin $D_{D,wall}$	1.70 x $10^{-11} m^2/s$	Experimental data for similar stainless steel filters	[15]
Diffusivity of drug in SBF $D_{D,SBF}$	4.22 x $10^{-10} m^2/s$	Diffusion of Linezolid in water	[21]
SBF Parameters			
SBF concentration at swelling point inside the matrix $C_{SBF,eq}$	29816.1 mol/m^3	Porosity of matrix * Density of SBF	
Diffusivity of SBF in the equilibrium swollen state of the system $D_{SBF,eq}$	5.6 x $10^{-10} m^2/s$	Experimental data from drug-eluting HPMC tablets	[14]
Diffusivity of SBF through the porous steel wall of the pin $D_{SBF,wall}$	8.1 x $10^{-11} m^2/s$	Interpolated from experimental data for similar solution in similar porous stainless steel	[15]
Constants			
Constants that represent concentration dependence (1 and 2)	2.5 and 9.5	Experimental data from drug-eluting HPMC tablets	[14]
Porosity of Drug Matrix	0.5236	Assumed silica beads were tightly packed, and calculated	[8]
Porosity of Porous Steel Wall	17%	Based on Prototype	[8]
Drug concentration in SBF far from the pin $C_{D\infty}$	0 mol/m^3		
Molar mass of SBF	18.01528 g/mol	Approximated as water	
Outside concentration of SBF C_{SBF}	1025 kg/m^3 56869 mol/m^3	Calculated based on experimental data	[22], [23]
Dynamic viscosity of SBF (μ_{SBF})	1.5 mPa*s	Blood plasma viscosity since SBF mimics blood plasma and is said to have similar a viscosity value	[24]
Speed of SBF outside the pin (u_{SBF})	1.5 x $10^{-6} m/s$	Used in experiment	[25]
Mass transfer coefficient of drug in SBF (h)	1.3504 x10^{-7} m/s	Calculated using aforementioned constants for convective flow over the cylinder	

Appendix B: Solution Strategy

B1. Computational Methods

This COMSOL model used time-dependent solver, PARDISO, to solve the algebraic equation. Since drug release is a transient process, the Backward Differentiation Formula (BDF) was used for time stepping, with a minimum order of 1 and a maximum order of 2. This model allows for an absolute tolerance of 0.1, and a relative tolerance of 0.01. For example, at time point six hours following implantation, the maximum error allowed in the drug concentration at the surface of the pin is (0.1 + 0.001*C_D) mol/m^3, where C_D is the concentration of the drug at that time.

B2. Mesh

Our mesh was built using the mapped mesh function with two distributions. Since the geometry of our model was fairly simple, we did not have to develop a complicated mesh for our calculations. Our mesh is shown in the figure below:

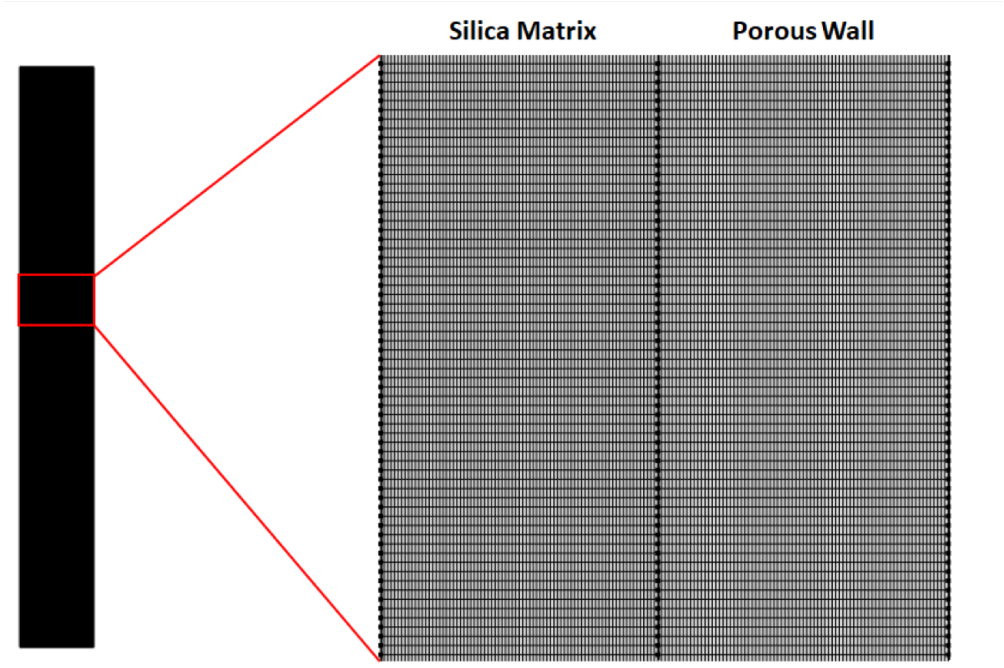

Figure 10: Mapped mesh with the silica matrix domain on the left connected with the porous wall domain on the right.

A mesh convergence was performed to assure that the results obtained by the simulation were independent of mesh. To accomplish this, the number of elements were increased until the computed concentration of drug in cut point 2 on the outside of the porous steel wall at five hours was fairly constant. We chose to carry out the mesh convergence at this point because the drug concentration at this point is what controls the bacterial growth. We chose the time point five hours because the first six hours are critical to control bacterial growth and the concentration at this time point should

not be dependent on the number of mesh elements. The solution converged at approximately 40,000 mesh elements per domain, as can be seen in the figure below:

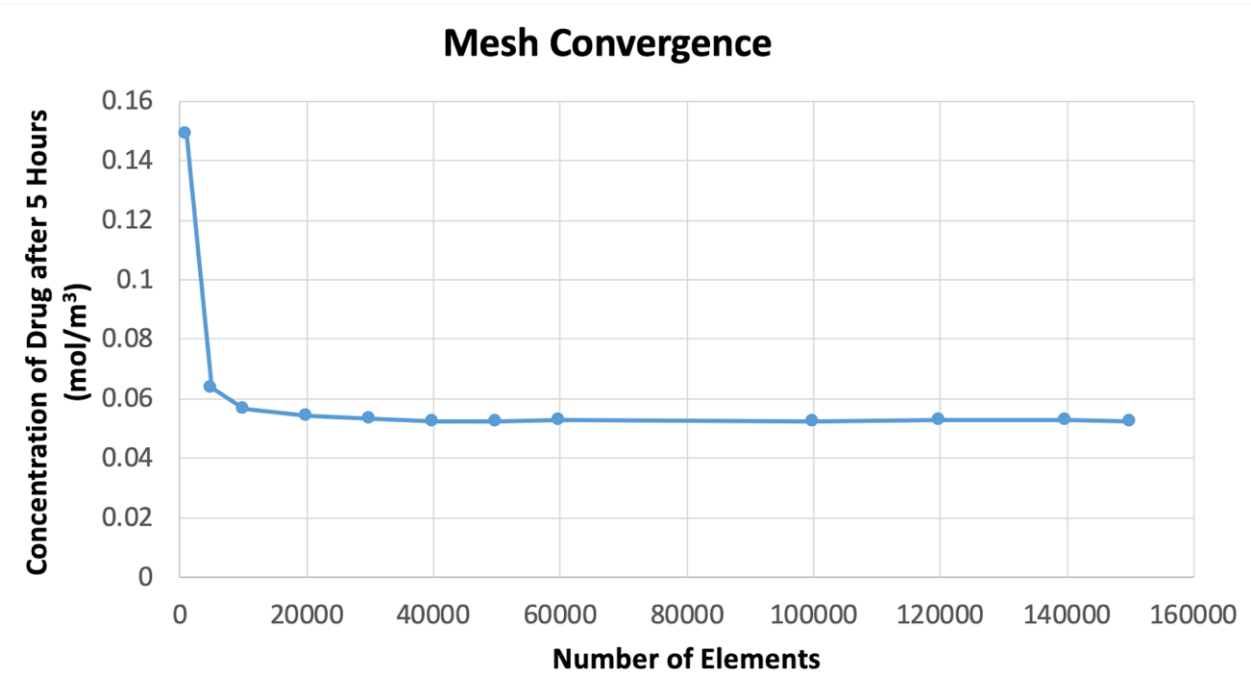

Figure 11: Mesh convergence graph showing drug concentration variation based on number of mesh elements per domain.

The resulting mesh at the point of convergence had a total of 80,000 elements, 80,661 mesh vertices, 1820 edge elements, 6 vertex elements, with a minimum and average element quality of 1.0, and 161322 degrees of freedom (DOF), with 4656 internal DOFs.

B3. CPU time taken and memory used by a typical run

For our mesh with 80,000 elements, the total time taken to compute the solution was 8 minutes and 36 seconds. 1.68 GB of physical memory was used and 1.9 GB of virtual memory was used during this calculation. This is summarized in the screenshot taken from COMSOL below:

```
Time-stepping completed.
Solution time: 516 s. (8 minutes, 36 seconds)
Physical memory: 1.68 GB
Virtual memory: 1.9 GB
Ended at 6-May-2019 15:23:04.
----- Time-Dependent Solver 1 in Study 1/Solution 1 (sol1) ---------------------->
================================================================================
```

Figure 12: Time taken and memory used for a typical run to obtain the solution.

Appendix C: Parameter Calculations

1. Diffusivity of SBF through the porous steel wall of the pin ($D_{SBF,wall}$)

The diffusivity of SBF through the porous steel wall of the pin, $D_{SBF,wall}$, was calculated by interpolating data based on SBF composition [15]. SBF contains mostly Na^+ and Cl^- in a 1:1 ratio, so the value of $D_{SBF,wall}$, was calculated by averaging the De values for the Na^+ solution and the Cl^- solution [15].

$$D_{SBF,wall} = \frac{1}{2}(D_{e,Na} + D_{e,Cl}) \tag{17}$$

$$D_{SBF,wall} = 8.1 * 10^{-11} m^2/s$$

Here, $D_{e,Na}$, the effective diffusivity of Na^+ solution in porous stainless wall with 19% porosity, is 6.5 x $10^{-11}10^{-11} m^2/s$. $D_{e,Cl}$, the effective diffusivity of Cl^- solution in the same porous stainless wall, is 6.5 x $10^{-11} m^2/s$. The calculated diffusivity of SBF through the porous steel wall of the pin was 8.1 x $10^{-11} m^2/s$.

2. Diffusivity of linezolid through the porous steel wall of the pin ($D_{D,wall}$)

The diffusivity of linezolid through the porous steel wall of the pin, $D_{D,wall}$, was calculated using the effective diffusivity equation from literature [15]:

$$D_e = \frac{\varepsilon}{G} D_w \tag{18}$$

In the case of our project, ε, the porosity of the wall, is 0.17. The overall geometric factor, G, is 4.2, adopted from Aldaba's experimental results [15]. The bulk diffusion coefficient of linezolid in SBF, D_w, is 4.22 x $10^{-10} m^2/s$. Therefore, we obtained that the diffusivity of Linezolid through the porous steel wall to be 1.70 x $10^{-11} m^2/s$.

3. Concentration of SBF (C_{SBF})

The concentration of SBF outside the pin (C_{SBF}) was calculated assuming the molecular weight of SBF was equivalent to the molecular weight of water, MW_{water} = 18.01528 g/mol. Because the density of SBF is similar to that of the blood serum, the density of the blood serum was used as ρ_{SBF}=1025000 g/m^3. Therefore, we obtained Equation 11.

$$C_{SBF} = \frac{\rho_{SBF}}{MW_{water}} \tag{11}$$

The concentration of SBF outside the pin (C_{SBF}) was calculated to be 56869.15 mol/m^3, or 1025 kg/m^3.

4. Initial concentration of the drug inside the silica beads (C_{Di})

The Initial concentration of the drug inside the silica beads (C_{Di}) was calculated based on the experimental parameters designed by Perez et al [8]. The total mass of drug inside the silica matrix, mD, is 3.515 mg. The molecular weight of linezolid, MW_D, is 337.351 g/mol. The volume of the matrix, V_m, is 185.5766 mm^3. The molecular weight of linezolid, MW_D, is 337.351 g/mol [8]. The value of C_{Di} was calculated as:

$$C_{Di} = \frac{m_D}{MW_D V_m} \tag{20}$$

Therefore the initial concentration of the drug inside the silica beads (C_{Di}) was found to be 56.0146 mol/m^3.

5. Mass transfer coefficient of drug in SBF (h)

Under the condition of forced convective flow over a cylindrical surface, the mass transfer coefficient of drug in SBF was calculated, using the Equation 21.

$$h = \frac{Sh_SBF * D_{D,SBF}}{d} \tag{21}$$

The diameter of the pin, d, is 6.25 x 10^{-3} m. The diffusivity of drug in SBF ($D_{D,SBF}$) is 4.22 x 10^{-10} m^2/s. The Sherwood number (Sh_{SBF}) is the ratio of molecular mass transport resistance to the convective mass transport resistance of the SBF. It is quantitatively defined in Equation 22.

$$Sh_{SBF} = B * Re_{SBF}^n * Sc^{1/3} \tag{22}$$

The Reynolds number (Re_{SBF}) of SBF flow was calculated using Equation 23.

$$Re_{SBF} = \frac{u_{SBF} * d * C_{SBF}}{\mu} \tag{23}$$

Here, the velocity of the SBF outside (μ_{SBF}) is 1.5 x 10^{-6} m/s. The density of SBF (C_{SBF}) is 1025 kg/m^3 [22,23]. The dynamic viscosity of SBF (μ_{SBF}) is 1.5 $mPa*s$ [24]. Plugging in these values, we found that the Reynolds number for SBF flow is 1.3504 x 10^{-3} m/s. The very small value for the Reynolds number suggests that the speed of fluid flow is so small that we can take it to be almost stagnant. In this case, the value of Sherwood's number can be approximated to be 2. Using the newly found Sherwood's number to solve for h, we obtained the mass transfer coefficient of drug in SBF (h) to be 1.3504 x 10^{-7} m/s.

Appendix D: References

[1] D. P. Lew, F. A. Waldvogel, "Osteomyelitis." Lancet, vol. 364, no. 9431, pp. 369-379, 2004.

[2] D. E. Reichman and J. A. Greenberg, "Reducing surgical site infections: a review," Reviews in Obstetrics & Gynecology, vol. 2, no. 4, pp. 212-221, 2009.

[3] C. Bibbo and J. Brueggeman, "Prevention and Management of Complications Arising from External Fixation Pin Sites," The Journal of Foot and Ankle Surgery, vol. 49, no. 1, pp. 87–92, 2010.

[4] K. A. Poelstra, N. A. Barekzi, A. M. Rediske, A. G. Felts, J. B. Slunt, and D. W. Grainger, "Prophylactic treatment of gram-positive and gram-negative abdominal implant infections using locally delivered polyclonal antibodies," Journal of Biomedical Materials Research, vol. 60, no. 1, pp. 206–215, 2002.

[5] L. Bernard, "Trends in the treatment of orthopaedic prosthetic infections," Journal of Antimicrobial Chemotherapy, vol. 53, no. 2, pp. 127–129, 2004.

[6] T. F. Moriarty, R. Kuehl, T. Coenye, W.-J. Metsemakers, M. Morgenstern, E. M. Schwarz, M. Riool, S. A. Zaat, N. Khana, S. L. Kates, and R. G. Richards, "Orthopaedic device-related infection: current and future interventions for improved prevention and treatment," EFORT Open Reviews, vol. 1, no. 4, pp. 89–99, 2016.

[7] M. Ribeiro, F. J. Monteiro, and M. P. Ferraz, "Infection of orthopedic implants with emphasis on bacterial adhesion process and techniques used in studying bacterial-material interactions," Biomatter, vol. 2, no. 4, pp. 176–194, 2012.

[8] L. M. Perez, P. Lalueza, M. Monzon, J. A. Puertolas, M. Arruebo, and J. Santamaría, "Hollow porous implants filled with mesoporous silica particles as a two-stage antibiotic-eluting device," International Journal of Pharmaceutics, vol. 409, no. 1-2, pp. 1–8, 2011.

[9] M. Zilberman, A. Kraitzer, O. Grinberg, and J. J. Elsner, "Drug-Eluting Medical Implants," Drug Delivery Handbook of Experimental Pharmacology, vol. 197, pp. 299–341, 2010.

[10] Z. Ruszczak and W. Friess, "Collagen as a carrier for on-site delivery of antibacterial drugs," Advanced Drug Delivery Reviews, vol. 55, no. 12, pp. 1679–1698, 2003.

[11] M. Gimeno, P. Pinczowski, M. Pérez, A. Giorello, M. Á. Martínez, J. Santamaría, M. Arruebo, and L. Luján, "A controlled antibiotic release system to prevent orthopedic-implant associated infections: An in vitro study," European Journal of Pharmaceutics and Biopharmaceutics, vol. 96, pp. 264–271, 2015.

[12] D. King and S. Mcginty, "Assessing the potential of mathematical modelling in designing drug-releasing orthopaedic implants," Journal of Controlled Release, vol. 239, pp. 49–61, 2016.

[13] K. Apostolos, J. Bryan, S. Taheri, "Molecular Diffusion", in Fundamentals of Fluid Flow in Porous Media.

[14] J. Siepmann, K. Podual, M. Sriwongjanya, N. Peppas, and R. Bodmeier, "A New Model Describing the Swelling and Drug Release Kinetics from Hydroxypropyl Methylcellulose Tablets," Journal of Pharmaceutical Sciences, vol. 88, no. 1, pp. 65–72, 1999.

[15] D. Aldaba, M. Glaus, O. Leupin, L. V. Loon, M. Vidal, and A. Rigol, "Suitability of various materials for porous filters in diffusion experiments," Radiochimica Acta, vol. 102, no. 8, 2014.

[16] D. T. Reilly and A. H. Burstein, "The elastic and ultimate properties of compact bone tissue," Journal of Biomechanics, vol. 8, no. 6, pp. 393–405, 1975.

[17] E. A. Lewallen, S. M. Riester, C. A. Bonin, H. M. Kremers, A. Dudakovic, S. Kakar, … A. J. van Wijnen, "Biological strategies for improved osseointegration and osteoinduction of porous metal orthopedic implants," Tissue engineering. Part B, Reviews, vol. 21. no. 2, pp. 218–230, 2014

[18] G. Harasen, "Orthopedic hardware and equipment for the beginner. Part 2: Plates and screws", PubMed Central (PMC), vol. 52, no. 12. pp. 1359-1360, 2019.

[19] O. Pieske, P. Geleng, J. Zaspel, and S. Piltz, "Titanium Alloy Pins Versus Stainless Steel Pins in External Fixation at the Wrist: A Randomized Prospective Study," The Journal of Trauma: Injury, Infection, and Critical Care, vol. 64, no. 5, pp. 1275–1280, 2008.

[20] W. Metsemakers, T. Schmid, S. Zeiter, M. Ernst, I. Keller, N. Cosmelli, D. Arens, T. F. Moriarty, and R. G. Richards, "Titanium and steel fracture fixation plates with different surface topographies: Influence on infection rate in a rabbit fracture model," Injury, vol. 47, no. 3, pp. 633–639, 2016.

[21] E. Bednarek, W. Bocian, and K. Michalska, "NMR and molecular modeling study, as complementary techniques to capillary electrophoresis method to elucidate the separation mechanism of linezolid enantiomers," Journal of Chromatography A, vol. 1193, no. 1-2, pp. 164–171, 2008.

[22] T. Kokubo, H. Kushitani, S. Sakka, T. Kitsugi, and T. Yamamuro, "Solutions able to reproduce in vivo surface-structure changes in bioactive glass-ceramic A-W3," Journal of Biomedical Materials Research, vol. 24, no. 6, pp. 721–734, 1990.

[23] A. Datta and V. Rakesh, An introduction to modeling of transport processes. New York: Cambridge University Press, 2010.

[24] "More News," Association for Clinical Biochemistry and Laboratory Medicine. [Online]. Available: http://www.acb.org.uk/.

[25] W. Yao, Y. Li, and G. Ding, "Interstitial Fluid Flow: The Mechanical Environment of Cells and Foundation of Meridians," Evidence-Based Complementary and Alternative Medicine, vol. 2012, pp. 1–9, 2012.